Impact of Increased Penetration of Fixed Speed Wind Generators on Power System Transient Stability

Amroune Mohammed *, Sebaa Haddi ** and Bouktir Tarek ***

Department of Electrical Engineering, SETIF University,
* amrounemohammed@yahoo.fr, ** Sebaa_73@yahoo.fr, *** tbouktir@gmail.com

Abstract – **The high penetration of wind power systems in the electrical network has introduced new issues in the stability and transient operation of the grid. This paper provides an assessment of wind power effects on the transient stability of a power system. The wind generators considered are the squirrel cage induction generator (SCIG), which is a fixed speed. The numerical simulations on the IEEE-30 bus test system are conducted to discuss the influence of penetration level of SCIG based wind generators on power system transient stability.**

Keywords – squirrel cage induction generator (SCIG), wind Generator, Transient stability, Wind generator.

I. INTRODUCTION

Recently due to the incremental rate of environmental concern, electrical energy generation using wind power has received much interest considerable attention all over the world. A huge number of wind farms are going to be connected with the existing network in the near future. Wind generators are primarily classified as fixed speed or variable speed. Due to its low maintenance cost and simple construction, induction generator is mostly used for wind power generation [1].

One of important issues engineers have to face is the impact of wind power penetration on the transient stability of an existing interconnected large-scale power system. Transient stability entails the evaluation of a power system's ability to withstand large disturbances and to survive the transition to another operating condition. These disturbances may be faults such as a short circuit on a transmission line, loss of a generator, loss of a load, gain of load or loss of a portion of transmission network [2]. A number of studies have been conducted on power system transient stability with high penetration, but they have considered simple network structures [3] [4] [5].

The objective of this paper is to investigate the impact of Fixed Speed wind generator penetration on power system transient stability. The numerical integration method is used to evaluate the transient stability and the IEEE-30 bus system is used as test case. The paper is organized as follows. Section II and III briefly introduces the mathematical models of power system and wind generator respectively. In section IV, the detail case studies focusing on the impacts of fixed speed grid-connected wind farms on IEEE-30 bus test system are carried out. Finally the conclusions are summarized in Section V.

II. POWER SYSTEM MODELING

The power system model consists of synchronous generator, transmission network and static load models, which are presented below.

The machine classical electromechanical model is represented by the following differential equations [6]:

$$\frac{d\delta_i}{dt} = \omega_i - \omega_s$$

$$\frac{d^2\delta_i}{dt^2} = \frac{\pi f}{H_i}\left(P_{mi} - P_{ei} - P_{Di}\right) \tag{1}$$

Where: $P_D = D\dfrac{d\delta}{dt}$

D is the generator damping coefficient; H is the inertia constant of machine expected on the common MVA base; P_m is the mechanical input power and P_e is the electrical output.

The transmission network model is described by the steady-state matrix equation:

$$I = YV \tag{2}$$

Where I is the injections current vector to the network, V is the nodal voltages vector and Y is the nodal matrix admittance.

The electrical power of the ith generator is given by [7]:

$$P_{ei} = E_i^2 G_{ii} + \sum_{j=1}^{ng} C_{ij} \cos\left[\theta_{ij} - \delta_i + \delta_j\right] \tag{3}$$

Where i = 1, 2, 3…ng is the number of generators.
$C_{ij} = |E_i||E_j||Y_{ij}|$ is the power transferred at bus ij;
E is the magnitude of the internal voltage;
Y_{ij} are the internal elements of matrix Y;
G_{ii} are the real values of the diagonal elements of Y.

The static model of load is represented by admittance Y defined by [7]:

$$Y_i = \left(\frac{P_i - jQ_i}{V_i^2}\right) \tag{4}$$

III. WIND GENERATOR MODELING

The fixed-speed, squirrel cage induction generator (SCIG) is connected directly to the distribution grid through a transformer. There is a gear box which maces the generator's speed to the frequency of the grid.

During high wind speeds, the power extracted from the wind is limited by the stall effect of the generator. This prevents the mechanical power extracted from the wind from becoming too large. In most cases, a capacitor bank is connected to the fixed speed wind generator for reactive power compensation purposes. The capacitor bank minimizes the amount of reactive power that the generator draws from the grid [2], (see figure 1).
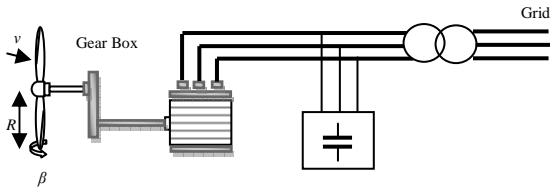

Fig. 1 Representation of the fixed speed induction generator

The model for the fixed speed synchronous generator is shown in Fig.2. Where R_s represents the stator resistance, X_s represents the stator reactance; X_m is the magnetizing reactance, while R_r and X_r represent the rotor resistance and reactance, respectively.
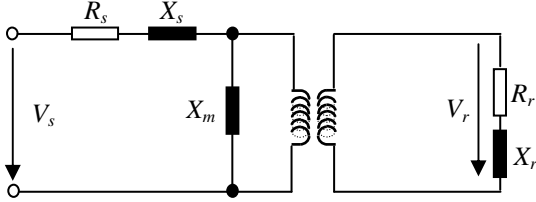

Fig. 2 Asynchronous machine equivalent circuit model

A standard detailed two-axis induction machine model is used to represent the induction generator. The relationship between the stator voltage, rotor voltage, the currents and the fluxes are given by the following equations [8]:

$$\begin{cases} v_{ds} = -R_s \times i_{ds} - \omega_s \times \lambda_{qs} + \dfrac{d}{dt}\lambda_{ds} \\ v_{qs} = -R_s \times i_{qs} + \omega_s \times \lambda_{ds} + \dfrac{d}{dt}\lambda_{qs} \end{cases} \quad (5)$$

$$\begin{cases} v_{dr} = 0 = R_r \times i_{dr} - g \times \omega_s \times \lambda_{qr} + \dfrac{d}{dt}\lambda_{dr} \\ v_{qr} = 0 = R_r \times i_{qr} + g \times \omega_s \times \lambda_{dr} + \dfrac{d}{dt}\lambda_{qr} \end{cases} \quad (6)$$

Where V_s is the stator voltage while V_r represents the rotor voltage, λ_s and λ_r are the stator and rotor flux

respectively, while ω_s is the synchronous speed. The rotor voltage is zero because the rotor has been short-circuited in the single cage induction generator. The model is completed by the mechanical equation as given below:

$$\frac{d\omega_r}{dt} = \frac{1}{2H} \times (T_m - T_e) \quad (7)$$

H is the inertia constant; T_m is the mechanical torque; T_e is the electrical torque and ω_r is the generator speed.

IV. SIMULATION RESULTS

Simulation studies are carried out in this section to demonstrate the transient performance of the power system with wind power integration. The Critical Clearing Time (CCT) is used as indices to evaluated transient stability and the IEEE 30-bus test system shown in fig. 3 is employed to conduct the transient stability simulation. Detailed parameters of this system can be found in [9]. A wind farm based on Fixed Speed Induction Generator (FSIG) is used and the FSIG parameters are outlined in the Appendix.
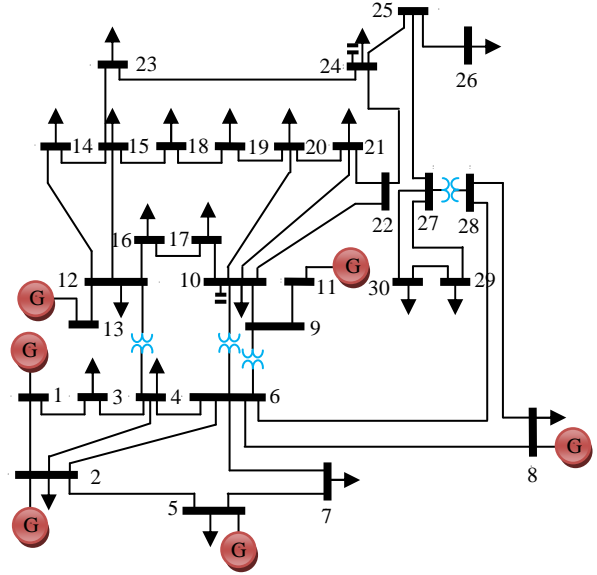

Fig. 3 Single line diagram of the IEEE 30-bus system

The test system is analyzed using optimal power flow (OPF). A standard OPF problem can be formulated as follows [10] [11]:

$$F(x) = \sum_{i=1}^{ng} (a_i + b_i P_{gi} - c_i P_{gi}^2) \quad (8)$$

$$P_i(V, \theta) + P_{di} - P_{gi} = 0 \quad (9)$$

$$Q_i(V, \theta) + Q_{di} - Q_{gi} = 0 \quad (10)$$

$$P_{gi}^{min} \leq P_{gi} \leq P_{gi}^{max} ; i=1,...ng \quad (11)$$

$$Q_{gi}^{min} \leq Q_{gi} \leq Q_{gi}^{max} ; i=1,...ng \quad (12)$$

Where F(x) is a cost function; a_i, b_i, c_i are cost coefficients shown in the Appendix; P_{gi} and Q_{gi} are the active and reactive power generations at i^{th} bus; P_{di} and Q_{di} are the active and reactive power demands at i^{th} bus; P_i and Q_i are the active and reactive power injections at i^{th} bus.

A. Case 1: Single FSGI wind farm

In this case the FSIG wind farm of 20 MW has been connected to bus 10 and bus 24 separately. The Optimal Power Flow results obtained with used of the Differential Evolution Algorithm (DEA) [12] [13] with and without of wind farm is listed in Table I. According to this table connecting the wind farm at bus 24 will be a better option in terms reduction in the total costs and power losses.

TABLE I
OPF RESULTS WITH DEA

BUS №	P_G (MW) Without WF	P_G (MW) With WF at bus 10	P_G (MW) With WF at bus 24
1		167.0748	167.0383
2		46.4729	46.4601
5		20.7535	20.7448
8		15.9062	15.8131
11		10.0000	10.0215
13		12.0000	12.0000
P loss		**8.80743**	**8.67769**
Total cost ($/h)		**741.518**	**741.072**

A disturbance in the form of a three phase to ground fault is occurs at t = 1 second at bus 1, cleared by opening the line connecting the nodes 1–2. The Figures 3 and 4 show the dynamic responses of all machines for Fault Clearing Time (FCT) equal to 170 ms and 213 ms respectively.
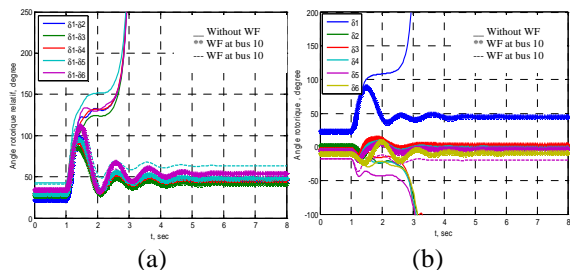

(a)   (b)

Fig. 4 Dynamic responses of all machines (FCT=170 ms)
(a) Rotor angle differences (b) Rotor angle
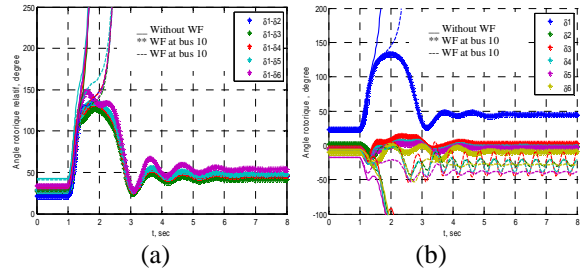

(a)   (b)

Fig. 5 Dynamic responses of all machines (FCT=213 ms)
(a) Rotor angle differences (b) Rotor angle

These Figures show that the Critical Clearing Time (CCT) increased after the introduction of the wind farm of FSIG type. For FCT = 213 ms, the system with Wind Farm (WF) at bus 10 remains stable and can return to steady state finally. However, the system with WF at bus 24 is unstable. Another's simulations have been performed for different fault locations in IEEE-30 bus system, in order to know the effect of FSIG wind farm location on transient stability. The results from the cases study are presented in Table II and Figure 6. The comparative results have shown that the location of wind turbines has an effect in transient stability of power system. In our case the insertion of a wind farm at bus 10 is better than its insertion at bus 24.

TABLE II
CCT WITH AND WITHOUT OF FSIG WF

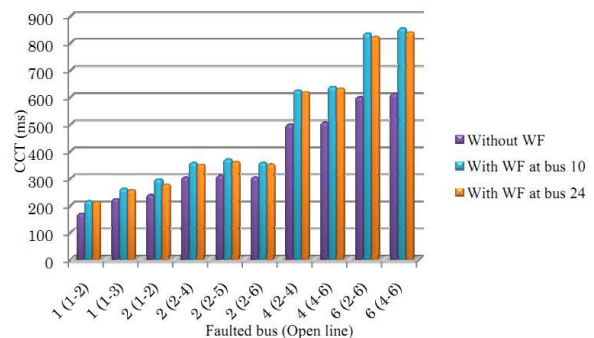| Faulted bus	Open line	CCT (ms) without WF	CCT (ms) with WF at bus 10	CCT (ms) with WF at bus 24
1	1 - 2	169	216	211
1	1 - 3	223	261	256
2	1 - 2	238	296	277
2	2 - 4	303	357	350
2	2 - 5	309	370	360
2	2 - 6	303	357	351
4	2 - 4	498	624	618
4	4 - 6	506	637	631
6	2 - 6	599	834	822
6	4 - 6	611	854	838

Fig. 6 CCT with and without of FSIG WF

To know the impact of wind penetration level on the power system Critical Clearing Time, the analysis has been carried out on 10%, 20%, 30% and 35% wind penetration levels based on the total power required (283.4 MW). The optimal active powers generated by all generators when FSIG wind farm is connected to bus 10 and to bus 24 are shown in Figures 7 and 8 respectively. The variation of CCT for the fault at bus 1 with opening the line 1–2 is shown in Figure 9. From these Figure, it can be seen that the system transient stability can be improved by improving penetration level of FSIG wind turbines.
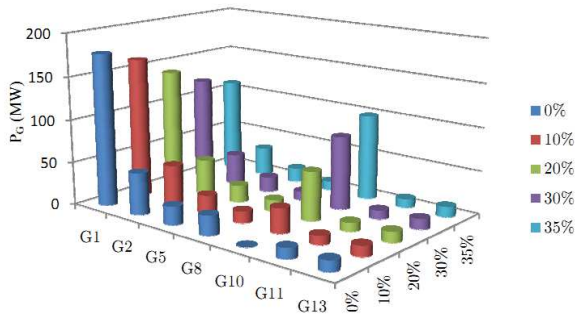

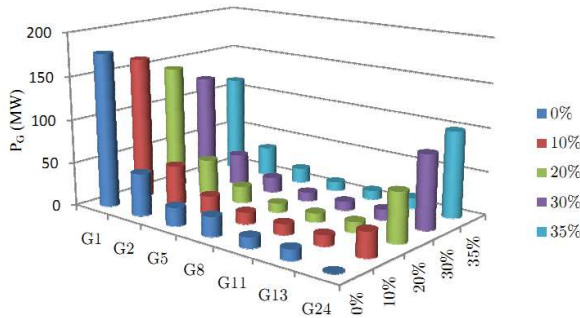Fig. 7 Power generation with FSIG WF connected at bus 10

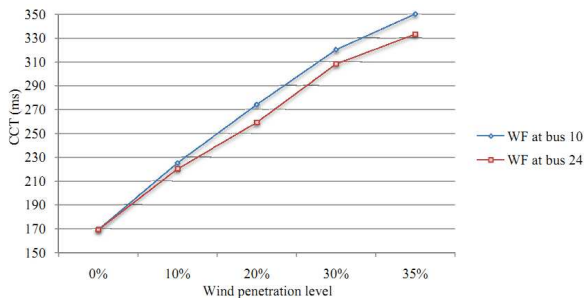Fig. 8 Power generation with FSIG WF connected at bus 24

Fig. 9 CCT variation with FSIG WF for a fault at bus 1

B. Case 2: Two FSIG wind farms

In this case the two FSIG wind farms have been connected to bus 10 and bus 24 simultaneously. Table III shown the total cost obtained with three penetration level scenarios. According to this table the total cost is low when the penetration level of wind farm is high at bus 10 and low at bus 24 (scenario 3).

TABLE III
OPF RESULTS WITH DEA

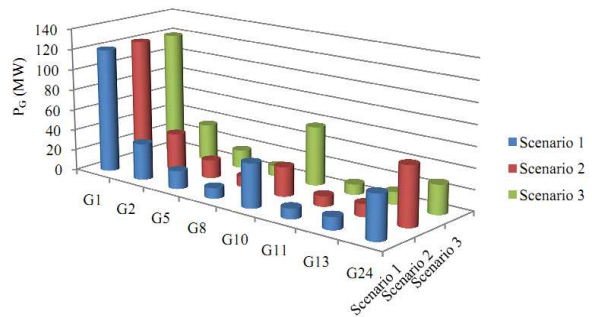|	G_{10}	G_{24}	Total cost ($/h)
Scenario 1	15%	15%	562.244
Scenario 2	10%	20%	664.419
Scenario 3	20%	10%	561.28

Fig. 10 Power generation for deferent scenarios

To get the impact of power distribution between two wind farms on transient stability, a three-phase short circuit has been simulated on deferent selected buses for the three previous scenarios. The results are shown in Table IV and Figure 11. The distribution of power between FSIG wind farms has an effect on transient stability of power system, in our study the CCT is more improved when the penetration level of wind farm is high at bus 10 and low at bus 24 (scenario 3).

TABLE IV
CCT FOR DEFERENT SCENARIOS

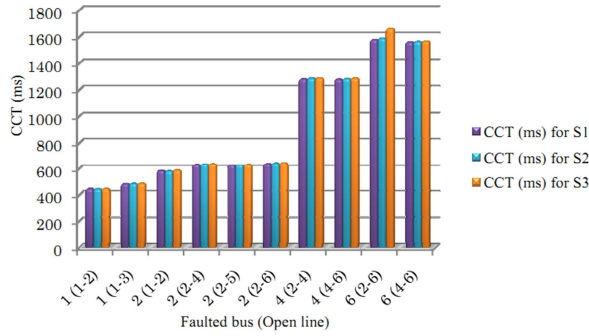| Faulted bus	Open line	CCT (ms) for S1	CCT (ms) for S2	CCT (ms) for S3
1	1 - 2	445	443	445
1	1 - 3	483	484	485
2	1 - 2	584	580	586
2	2 - 4	631	635	636
2	2 - 5	626	629	631
2	2 - 6	638	642	644
4	2 - 4	1281	1286	1288
4	4 - 6	1278	1283	1286
6	2 - 6	1576	1587	1659
6	4 - 6	1558	1561	1564

Fig. 11 CCT for deferent scenarios

VI. CONCLUSION

The impact of increased penetration of fixed speed wind generators on power system transient stability is discussed in this paper. The multiple wind farms integration is studied also. According to the simulation results, some preliminary conclusions and comments can be summarized as follows:

The addition of FSIG type wind generator to the power system improved the rotor angle transient stability;

The location and number of FSIG has an effect on transient stability of power system;

The increased of penetration level of wind generation FSIG type increase the power system Critical Clearing Time;

The distribution of power between FSIG wind farms has an effect on transient stability of power system.

REFERENCES

[1] M. Muyeen, et al., "Transient Stability Analysis of Wind Generator System with the Consideration of Multi-Mass Shaft Model," in *International Conference on Power Electronics and Drives Systems,PEDS.*, 2005, pp. 511-516.

[2] K. Folly, "Impact of Fixed and Variable Speed Wind Generators on the Transient Stability of a Power System Network," in *IEEE/PES Power Systems Conference and Exposition, 2009. PSCE '09.* , Univ. of Cape Town, Cape Town , 15-18 March 2009, pp. 1-7.

[3] S. Mohandas and A. Kumar, "Transient Stability Enhancement of the Power System with Wind Generation," *TELKOMNIKA*, vol. 9, no. 2, pp. 267-278, Aug. 2011.

[4] L. Shi, D. Ni, L. Yao, and M. Bazargan, "Transient stability of power system with high penetration of DFIG based wind farms," in *IEEE Power & Energy Society General Meeting, 2009. PES '09.* , Univ., Shenzhen, China, 26-30 July 2009, pp. 1-6.

[5] S. Sheri, B. Shankarprasad, V. Bhat, and S. Jagadish, "Effect of Doubly Fed Induction Gennerator on Transient Stability Analysis of Grid" *IEEE Transactions on Energy Conversion*, vol. 20, no. 2, p. 388–397, June 2005.

[6] P. K. Iyambo, "Transient stability analysis of the IEEE 14-bus electric power system," in *AFRICON 2007*, Cape Peninsula Univ. of Technol., Cape Town, 2007, pp. 1-9.

[7] P. Kundur, *Power System Stability and Control 1994* . New York: Mc Graw-Hill, 1994.

[8] L. Holdsworth, "Comparison of fixed speed and doubly-fed induction wind turbines during power system disturbances ," *IEE Proceedings-Generation, Transmission and Distribution*, vol. 150, no. 3, pp. 343-352, 2003.

[9] M. Iannone and F. Torelli, "Acoherency-basedmethod to increasedynamicsecurity in power systems," *Electric Power Systems Research*, vol. 78, no. 8, p. 1425–1436, Aug. 2008.

[10] T. Bouktir, L. Slimani, and M. Belkacemi, "A Genetic Algorithm for Solving the Optimal Power Flow Problem ," *Leonardo Journal of Sciences*, no. 4, pp. 44-58, Jan. 2004.

[11] P. Somasundaram and N. Muthuselvan, "a modified particle swarm optimization technique for solving transient stability constrained optimal power flow," *Journal of Theoretical and Applied Information Technology*, pp. 154-164, 2010.

[12] R. Storn, "Differential Evolution – A Simple and Efficient Heuristic for Global Optimization over Continuous Spaces," *Journal of Global Optimization*, p. 341–359, 1997.

[13] T. Bouktir and L. Slimani, "Optimal Power Flow Solution of the Algerian Electrical Network using Differential Evolution Algorithml," *TELKOMNIKA*, vol. 9, no. 1, pp. 1-8, Apr. 2011.

APPENDIX

A. Power generation limits and cost coefficients

BUS №	Cost Coefficients			P_G^{MIN} (MW)	P_G^{MAX} (MW)
	a	*b*	*c*		
1	0	2	0.00375	50	200
2	0	1.75	0.0175	20	80
5	0	1	0.0625	15	50
8	0	3.25	0.0083	10	35
11	0	3	0.025	10	30
13	0	3	0.025	12	40

B. Induction wind turbine model parameters

Stator resistance (R_s): 0.1015 pu

Rotor resistance (R_r): 0.0880 pu

Stator reactance (X_s): 3.5547 pu

Rotor reactance (X_r) : 3.5859 pu

Magnetizing reactance (X_m): 3.5092 pu

Inertia constant (H): 4 s; S_{base} = 5 MVA